First-principles study of the spin-gap system $Sr_2Cu(BO_3)_2$

Jayita Chakraborty and Indra Dasgupta*

Department of Solid State Physics and Center for Advanced Materials, Indian Association for the Cultivation of Science, Jadavpur, Kolkata 700032, India

(Received 9 February 2012; revised manuscript received 7 August 2012; published 20 August 2012)

We have employed first-principles electronic structure calculations based on the *N*th-order muffin-tin orbital downfolding method to derive a low energy spin model for the spin-gap compound $Sr_2Cu(BO_3)_2$. Our calculations reveal that this compound is a coupled dimer system with the strongest Cu-Cu interaction mediated by a pair of BO_3 triangular units. The appreciable interdimer interactions are mediated via super-super exchange due to short O-O distances in the exchange pathway. The validity of the model is checked by calculating the magnetic susceptibility as a function of temperature and magnetization both as a function of temperature as well as field using quantum Monte Carlo technique and comparing them with the available experimental data. This comparison establishes the suitability of the coupled dimer model for the description of the low energy physics of $Sr_2Cu(BO_3)_2$.

DOI: 10.1103/PhysRevB.86.054434 PACS number(s): 71.20.−b, 75.30.Et, 75.10.Jm

I. INTRODUCTION

Low dimensional quantum spin systems continue to enjoy considerable attention both theoretically as well as experimentally due to the wealth of fascinating properties exhibited by them.[1] Of particular importance are systems that exhibit spin gap.[2] Exotic features related to the ground state and excitations of such gapped systems form a subject matter of current interest. Copper based compounds have received a special interest due to their proximity to the superconducting two-dimensional cuprates. In this respect Cu based borates also attracted considerable attention. In particular, the quasi-two-dimensional spin $S = 1/2$ compound $SrCu_2(BO_3)_2$[3] was suggested to be the experimental realization of the Shastry-Sutherland[4] model exhibiting spin-gap behavior and magnetization plateaus at 1/8, 1/4, and 1/3 of the saturated magnetization. Following this discovery, there have been attempts to tune the magnetic couplings in such systems upon proper substitutions in order to explore the rich phase diagram of the Shastry-Sutherland model. One such attempt has been the realization of $CdCu_2(BO_3)_2$ by replacement of Sr^{2+} by another divalent cation Cd^{2+}.[5] This compound exhibits long range magnetic order and 1/2 magnetization plateau. A recent theoretical work[6] uncovers that $CdCu_2(BO_3)_2$ is a possible realization of the spin 1/2 decorated anisotropic Shastry-Sutherland lattice.

In this borate family, the magnetic properties of the recently discovered spin-gap compound $Sr_2Cu(BO_3)_2$ is particularly intriguing.[7] The structure of $Sr_2Cu(BO_3)_2$ consists of CuO_4 square plaquettes and CuO_6 octahedra which are connected to each other by BO_3 triangular units and run along the crystallographic c direction as illustrated in Fig. 1. This composition is very similar to the Shastry-Sutherland[4] compound $SrCu_2(BO_3)_2$,[8] but it has a very different magnetic lattice and the high field and low temperature magnetic behavior is particularly interesting. The magnetization data[7] for $Sr_2Cu(BO_3)_2$ at low field is consistent with the fact that the material has a singlet ground state comprising of dimers, with intradimer coupling $J \approx 100$ K. As expected in the presence of higher applied field the triplet excitations are observed. Interestingly, the applied field where excitation of singlet into triplet state takes place is found to be significantly smaller than that predicted for the isolated dimers. This in turn indicated that the interdimer couplings may be important and possibly responsible for the triplet states at smaller fields. The importance and the nature of the interdimer couplings are not always obvious from the structural considerations. It is therefore important to establish a connection between the underlying chemical complexity of the compound and the corresponding spin lattice. In this context *ab initio* electronic structure calculations have played an important role in analyzing and understanding such low dimensional quantum spin systems.[9–12]

In this paper, we shall examine the electronic structure of $Sr_2Cu(BO_3)_2$ in some detail and in particular identify the dominant exchange paths and the relevant spin Hamiltonian. This spin Hamiltonian will be employed to compute the magnetic susceptibility as a function of temperature and magnetization both as a function of field as well as temperature using quantum Monte Carlo simulation (stochastic series expansion).[13–16] We shall compare our results with available experimental data, in order to clarify the importance of the interdimer coupling as anticipated in the experiments. The remainder of this paper is organized as follows. In Sec. II we discuss the crystal structure and the computational details. Section III is devoted to the analysis of the electronic structure, derivation of the relevant spin Hamiltonian, and its solution using the QMC method. Finally, the summary and conclusions are given in Sec. IV.

II. CRYSTAL STRUCTURE AND COMPUTATIONAL DETAILS

$Sr_2Cu(BO_3)_2$ exists in two structural phases. The high temperature β-$Sr_2Cu(BO_3)_2$ phase studied here crystallizes in the orthorhombic space group P_{nma} with the lattice parameter $a = 7.612$ Å, $b = 10.854$ Å, and $c = 13.503$ Å.[17] All the electronic structure calculations in the present work are carried out using the lattice parameters and the atomic positions as reported in Ref. 17. The structure of $Sr_2Cu(BO_3)_2$ is shown in Fig. 1. The unit cell has eight formula units with 88 atoms in the unit cell as shown in Fig. 1(a). It has a

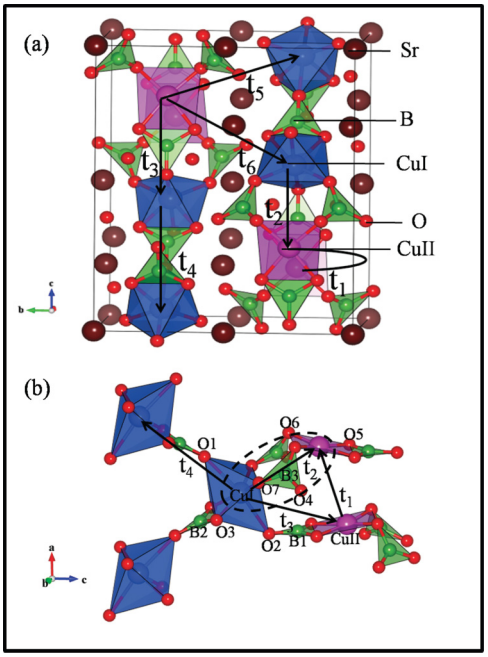

FIG. 1. (Color online) (a) Unit cell of $Sr_2Cu(BO_3)_2$. (b) One Cu(I) octahedron is connected with two $Cu(II)O_4$ square planar units and two other $Cu(I)O_6$ octahedra. The dimer unit is indicated by the dotted circle.

layered structure (*ac* plane), where each layer is built of distorted $Cu(I)O_6$ octahedra, square planar $Cu(II)O_4$ units, and triangular $B(1,2,3)O_3$ units, as shown in Fig. 1(b). This distorted $Cu(I)O_6$ octahedron has four inequivalent oxygens O1, O2, O3, and O7 surrounding each Cu(I) ion. Each $Cu(I)O_6$ octahedron is elongated along the O1-O2 axis, with distances $d_{Cu(I)\text{-}O1} = 2.42$ Å and $d_{Cu(I)\text{-}O2} = 2.49$ Å. The equilateral oxygens are at $d_{Cu(I)\text{-}O7} = 1.92$ Å and $d_{Cu(I)\text{-}O3} = 1.99$ Å. These layers are stacked along the crystallographic *b* axis with Sr ions in between them. As can be seen in Fig. 1(b), each $Cu(I)O_6$ octahedron is connected to two $Cu(I)O_6$ octahedra and a pair of square planar $Cu(II)O_4$ units with the aid of BO_3 triangular units. Among the two square planar units one is connected to the $Cu(I)O_6$ octahedron by a pair of BO_3 units and the Cu(I) and Cu(II) residing on the octahedral and square planar unit respectively defines the structural dimer, as indicated in Fig. 1(b).

In order to analyze the electronic structure of $Sr_2Cu(BO_3)_2$ we have carried out density functional theory (DFT) calculations within local density approximation (LDA) by employing the Stuttgart TB-LMTO-47 code,[18] based on the tight binding linearized muffin-tin orbital (TB-LMTO) method in the atomic sphere approximation (ASA). The space filling in the ASA is obtained by inserting appropriate empty spheres in the interstitial regions. For the TB-LMTO-ASA calculation the basis set for the self-consistent electronic structure calculation for $Sr_2Cu(BO_3)_2$ includes Sr(s,d), Cu (s,p,d), O(s,p), and B (s,p) and the rest are downfolded. A ($4 \times 2 \times 2$) k mesh has been used for self-consistency. In addition, the total energy calculations necessary for the evaluation of the exchange integrals are carried out in the plane wave basis along with the projected augmented wave (PAW)[19] method as implemented in the Vienna *ab initio* simulation package (VASP).[20] The exchange-correlation (XC) term in DFT was treated within the GGA due to Perdew-Burke-Ernzerhof (PBE).[21] We used a plane-wave energy cutoff of 500 eV and k-space sampling on a $4 \times 2 \times 2$ Monkhorst-Pack grid.

In order to derive a low energy effective model Hamiltonian that will serve as the single electron part of the many body Hamiltonian necessary to model the system, we have employed the Nth-order muffin-tin orbital (NMTO) downfolding method.[22–24] A strong on-site Coulomb interaction (U) is added to the noninteracting Hamiltonian obtained from the NMTO downfolding method to construct a Hubbard model for the many body description of $Sr_2Cu(BO_3)_2$. This model in the limit of half filling reduces to the Heisenberg model and thereby provides the necessary spin Hamiltonian. The resulting spin Hamiltonian has been solved to calculate susceptibility as a function of temperature and magnetization as a function of temperature and field using QMC with the aid of stochastic series expansion (SSE) algorithm.[13–16]

III. RESULTS AND DISCUSSIONS

A. Electronic structure and low energy model Hamiltonian

The non-spin-polarized band structure for $Sr_2Cu(BO_3)_2$ obtained by TB-LMTO ASA method is shown in Fig. 2. The bands are plotted along the various high symmetry points of the Brillouin zone corresponding to the orthorhombic lattice of $Sr_2Cu(BO_3)_2$. All the energies are measured with respect to the Fermi level of the compound. The characteristic feature of the band structure is the isolated manifold of eight bands crossing the Fermi level (E_F) which arises from the eight copper atoms in the unit cell. These eight bands are predominantly of Cu-$d_{x^2-y^2}$ character in the local frame of reference where Cu is at the origin and the x and y axis point along the oxygens residing either on the basal plane of the octahedron or the square planar unit. These isolated eight bands are responsible for the low energy physics of the material. These bands are half filled and separated from the

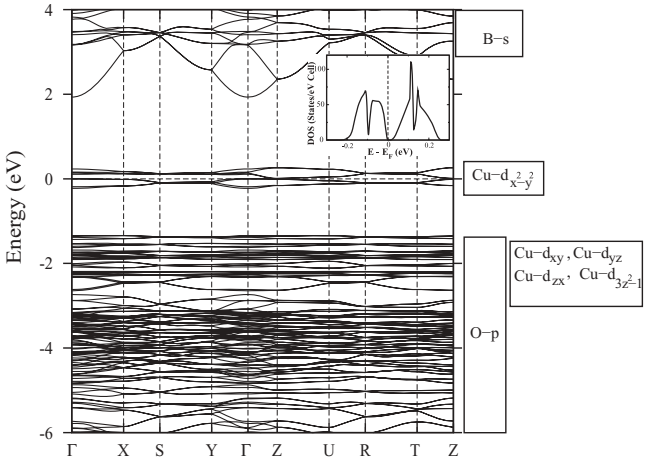

FIG. 2. LDA band structure of $Sr_2Cu(BO_3)_2$ plotted along various symmetry directions of the orthorhombic lattice. The zero of the energy has been set up at the LDA Fermi energy. The dominant orbital contributions in various energy ranges are shown in boxes on the right-hand side. Inset shows the total density of states close to the Fermi level.

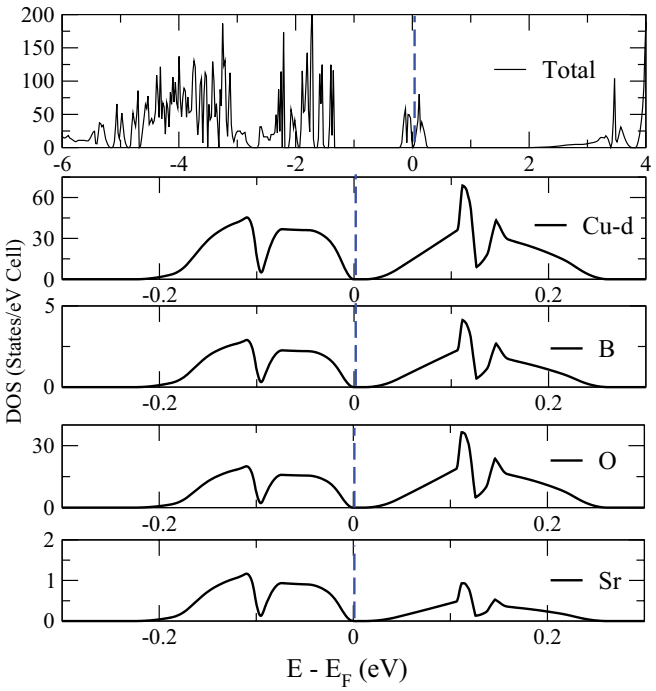

FIG. 3. (Color online) Total density of states of $Sr_2Cu(BO_3)_2$. Inset shows the partial density of states for Cu-d, B, O and Sr in the energy range close to E_F.

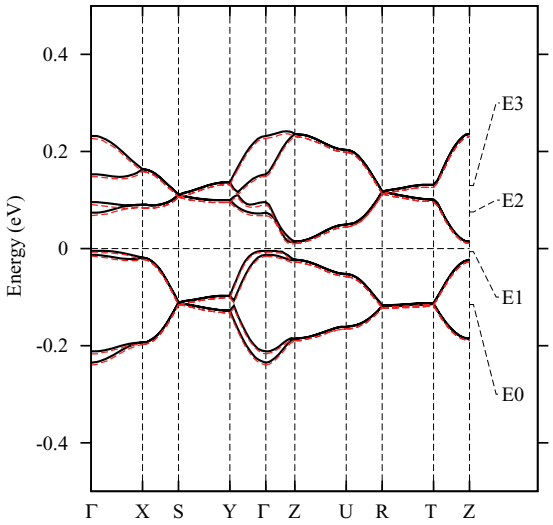

FIG. 4. (Color online) Downfolded band structure (shown in dotted line) compared to the full orbital band structure (shown in black line) for $Sr_2Cu(BO_3)_2$. E_0, E_1, E_2, E_3 mark the energy points used in the NMTO calculation.

low lying O p and other non-Cu-$d_{x^2-y^2}$ valence bands by a gap of about 1.8 eV. The system is insulating (see inset of Fig. 2) and the magnitude of the gap is calculated to be 10 meV in LDA indicating interactions in the Cu-$d_{x^2-y^2}$ manifold. Figure 3 displays the total DOS and the partial DOS contribution from Cu, B, O, and Sr near the Fermi level. We note that in addition to the Cu and oxygens the bands at the Fermi level have non-negligible admixture with the B states which are expected to participate in the superexchange process. In order to ascertain the accuracy of our ASA calculations we also performed the electronic structure calculation using a projected augmented wave (PAW)[19] method encoded in the Vienna *ab initio* simulation package (VASP).[20] The density of states calculated by these two different approaches are found to agree well with each other.

The Nth-order muffin-tin orbital (NMTO) downfolding method[22–24] has been established to be an efficient *ab inito* scheme to construct a low energy, few band, tight binding model Hamiltonian. This method generates the basis set which describes an isolated band or group of bands. The low energy model Hamiltonian is constructed by selective downfolding method via integration process. The high energy degrees of freedom are integrated out from the all orbital LDA calculations. The number of energy points (N) used for the downfolding technique is very important for the accuracy of the calculation. For an isolated set of bands, an atom centered and localized set of Wannier functions may be generated by symmetrical orthonormalization of the NMTOs.[25]

In order to extract the low energy model Hamiltonian, we have retained the isolated eight band complex near the Fermi level and downfolded the rest with the choice of four energy points E_0, E_1, E_2, and E_3. The downfolded bands in comparison to the all orbital LDA band structure is shown in Fig. 4 and we note that the agreement is remarkable. The Fourier transform of the low energy Hamiltonian $H_k \rightarrow H_R$ [where H_R is given by $H_R = \sum_{ij} t_{ij}(c_i^\dagger c_j + \text{H.c.})$] gives the effective hopping parameters between the various Cu atoms. The exchange interactions can be expressed as sum of antiferomagnetic (AFM) and ferromagnetic (FM) contributions $J = J^{\text{FM}} + J^{\text{AFM}}$. For strongly correlated systems, the antiferromagnetic contributions can be calculated by the following relation: $J_n^{\text{AFM}} = \frac{4t_n^2}{U_{\text{eff}}}$, where U_{eff} is the effective on-site Coulomb interaction and t_n corresponds to the hopping via superexchange paths. The various hopping integrals (>1 meV) extracted for $Sr_2Cu(BO_3)_2$ are listed in Table I and the notation is indicated in Fig. 1.

The various Cu-Cu hoppings in the a-c plane [see Fig. 1(b)] are primarily mediated via oxygens that are shared by the $Cu(I)O_6$ octahedra, $Cu(II)O_4$ square planar units, and the BO_3 units. The equitorial oxygens of an $Cu(I)_6$ octahedron (e.g., O3 and O7) hybridize strongly with the Cu(I)-$d_{x^2-y^2}$ orbital while the apical oxygens (O1 and O2) hardly hybridize with it. As a consequence the effective Cu-$d_{x^2-y^2}$–Cu-$d_{x^2-y^2}$ hopping is strong provided the equitorial oxygens of an octahedron are linked by B either to the oxygens in the square planar unit or to the equitorial oxygens of a neighboring octahedron. This is precisely the case for the structural dimer thereby accounting for its appreciable hopping, $t_2 = 112$ meV. The hopping t_3 and t_4 [see Fig. 1(b)] proceed with the aid of the apical oxygens and therefore are expected to be small. Our calculations indeed reveal that t_3 is negligible and $t_4 \approx 4$ meV. In addition to the above hoppings there is a small direct hopping t_1 between a pair of Cu(II) residing on neighboring square planar units, along crystallographic a axis.

Our above argument is further substantiated by a plot of Cu-$d_{x^2-y^2}$ Wannier function, where we have plotted the Cu-$d_{x^2-y^2}$ Wannier function for Cu(II) residing on the square planar unit and connected to the $Cu(I)O_6$ octahedron by

TABLE I. Hopping integrals and exchange interactions (in meV).

Types of Cu	Hopping	Cu-Cu distance (Å)	O-O distance (Å)	Hopping parameters (meV)	$J_i^{\mathrm{AFM}}/J_2^{\mathrm{AFM}} = (t_i/t_2)^2$	Total exchange interactions for $U = 6$ eV (meV)
Cu(II)-Cu(II)	t_1	4.03	3.39 (O5-O6)	13.6	0.015	0.25
Cu(I)-Cu(II)	t_2	4.27	2.37 (O6-O7)	112	1	−10.75
Cu(I)-Cu(I)	t_4	6.12	2.40 (O1-O3)	4.08	0.001	−0.60
Cu(I)-Cu(II)	t_5	6.25	3.07 (O7-O6)	40	0.127	−2.40
Cu(I)-Cu(II)	t_6	6.35	3.1 (O3-O5)	9.52	0.007	1.78

a pair of BO_3 units [see Fig. 5 (left)]. The plot reveals that the Cu(II)-$d_{x^2-y^2}$ orbital forms strong $pd\sigma$ antibonds with the neighboring O-p_x and O-p_y orbitals. From the tail of the Wannier function we find that it strongly hybridizes with the BO_3 network and also with the Cu(I)-$d_{x^2-y^2}$ orbital. This hybridization mediated by a pair of BO_3 units as argued above is responsible for the strong t_2 hopping. The plot of the Wannier function for the Cu(II) which is connected to Cu(I) by a single BO_3 unit via the apical oxygen [see Fig. 5 (right)] reveals that although Cu(II) hybridizes strongly with the BO_3 unit the tail of the Wannier function does not have any weight at the Cu(I) site because this hybridization is weak as it proceeds via the apical oxygen, thereby accounting for its negligible coupling.

In order to clarify the role of B in mediating the strong hopping t_2, we have plotted in Fig. 6 the Wannier function corresponding to B(3)-p_x in an energy range above the Fermi level belonging to the antibonding part of the B -O hybrid dominated by the B-p states. As expected the plot reveals that B(3) p_x orbital forms antibonds with the neighboring oxygens

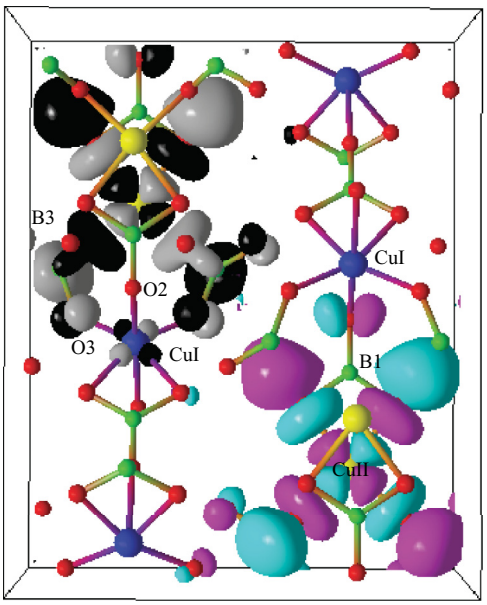

FIG. 5. (Color online) Wannier function of Cu-$d_{x^2-y^2}$, placed at two Cu(II) sites residing on the square planar units. One is connected to the Cu(I)O_6 octahedron by a pair of BO_3 units (in left) and the other Cu(II) is connected to the Cu(I)O_6 octahedron by one BO_3 unit (in right). Lobes of orbitals placed at different Cu(II) sites are colored differently.

in the triangular unit which in turn form an antibonding linear combination with Cu(I) and Cu(II). The main role of the B is to bring the oxygens together in the BO_3 unit and strengthen the intradimer coupling. The participation of B in the intradimer coupling is reflected by the appearance of finite weight both at the CuI and the CuII sites in the tail of the B(3)-p_x Wannier function.

Next we have considered the hoppings along the crystallographic b direction particularly t_5, which is the second largest interaction. Figure 7 shows the Wannier function plots of Cu-$d_{x^2-y^2}$ corresponding to t_5 hopping. From the Wannier function, we gather that the Cu-Cu interdimer hopping along the b direction primarily proceeds via oxygens. Although the Cu-Cu distance is large, the relatively strong hopping is due to short O-O distances (see Table I) (comparable to van der Waals distance) in the hopping pathway.[12] This hopping path will be responsible for the interdimer exchange interaction.

Table I reveals that the dominant hoppings (>10 meV) are t_1, t_2, and t_5. However, a tight binding (TB) analysis reveals that excluding t_1 a reasonable fit to the low energy NMTO band structure is obtained except for the small splitting along (ΓX), (S Y), and (R T) directions. Using second order perturbation expression $J_n^{\mathrm{AFM}} = \frac{4t_n^2}{U_{\mathrm{eff}}}$, the intradimer exchange interaction is calculated to be 12.5–10.03 meV, taking the standard value of $U_{\mathrm{eff}} = 4.0$–5.0 eV.[6,26] The ratio of the exchange integrals are listed in Table I, where we have $J_5^{\mathrm{AFM}} = 0.127 J_2^{\mathrm{AFM}}$, and as expected the other alternation parameters are negligibly small.

In addition to the above estimate for the AFM contribution to the exchange interactions, we have employed a complementary approach to calculate the total exchange interactions. We have performed total energy calculations in the framework of GGA + U[27] method for various ordered spin configurations.

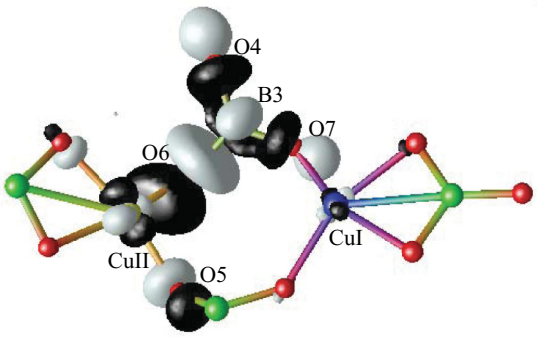

FIG. 6. (Color online) Effective orbital corresponding to the downfolded NMTOs, placed at B(3) site.

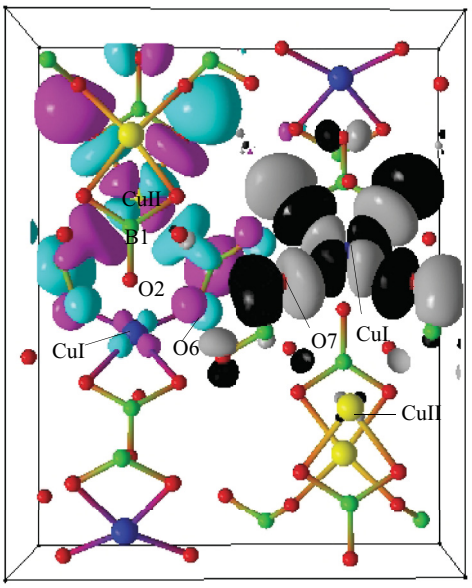

FIG. 7. (Color online) Effective orbital corresponding to the downfolded NMTOs, placed at Cu(I) and Cu(II) sites corresponding to the t_5 interaction. Lobes of orbitals placed at different Cu sites are colored differently.

In order to extract the various exchange interactions, the relative energies of these ordered spin state determined from the GGA + U calculations, are mapped onto the corresponding energies obtained from the total spin exchange energies of the Heisenberg spin Hamiltonian. For the GGA + U calculations the on-site Coulomb interaction (U) for Cu is taken to be $U = 6$ eV and the on-site exchange interaction $J = 1$ eV.[28,29] The results of our calculations are displayed in the last column of Table I. We gather from Table I that the dominant exchange interactions are J_2 and J_5 which are antiferromagnetic. J_1 and J_6 are weakly ferromagnetic. It is interesting to note that the estimate of J_2 and J_5 using the second order perturbation expression is -11.15 meV and -1.42 meV, respectively, for $U_{\text{eff}} = 4.5$ eV in good agreement with the exchange interactions obtained from the total energy calculations.

Table I reveals that the only relevant exchange interactions are the intradimer coupling J_2, and the interdimer exchange J_5. In contrast to our *ab initio* estimate, J_3 corresponding to hopping path t_3 and J_4 were anticipated to be the dominant interdimer exchange interactions based on structural considerations.[7] This in turn suggests that the identification of the exchange paths based on structural consideration may be deceptive and emphasizes the importance of *ab initio* calculations in identifying the dominant exchange paths.

The resulting spin model for $Sr_2Cu(BO_3)_2$ therefore turns out to be a system of coupled dimers as indicated in Fig. 8. The figure clearly reveals that the spin lattice is a system of decoupled spin ladders running along crystallographic b axis. The effective spin 1/2 Heisenberg model for the two leg ladder ($N \times 2$ lattice) may be written as

$$H = \sum_{i=1}^{N} J_2 \mathbf{S}_{i,1} \cdot \mathbf{S}_{i,2} + \sum_{i=1}^{N} \sum_{j=1,2} J_5 \mathbf{S}_{i,j} \cdot \mathbf{S}_{i+1,j}. \qquad (1)$$

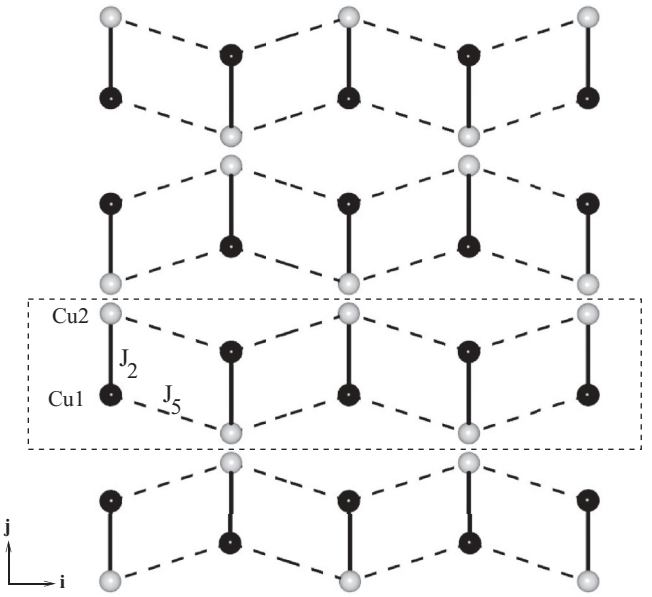

FIG. 8. Spin lattice of $Sr_2Cu(BO_3)_2$.

B. Susceptibility and magnetization

In order to check how the proposed spin model works, we have calculated the magnetic susceptibility as a function of temperature and magnetization both as a function of temperature and field and compared our results with the available experimental data.[7] We have used the stochastic series expansion (SSE) method to study the finite temperature properties of the Heisenberg antiferromagnet. The SSE is a finite-temperature QMC technique based on importance sampling of the diagonal matrix elements of the density matrix $\exp(-\beta\,\mathrm{H})$.[13–15] The susceptibility calculated by the SSE method is

$$\chi^{\text{th}} = \beta(\langle M^2\rangle - \langle M\rangle^2), \quad \text{with} \quad M = \sum_i S_i^z,$$

$$\chi = \frac{N g^2 \mu_B^2 \chi^{\text{th}}}{k_B J_2},$$

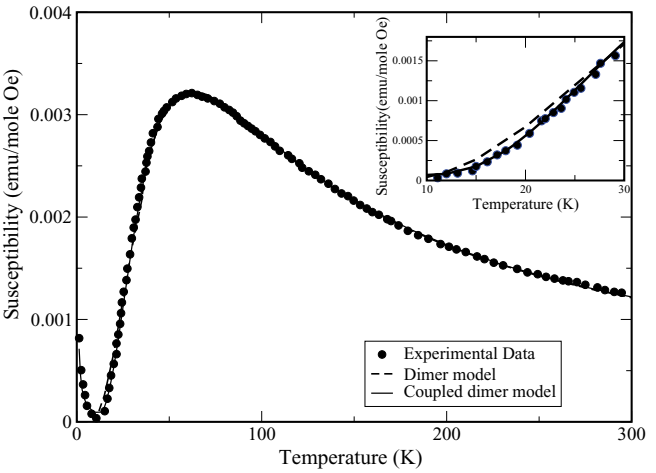

FIG. 9. (Color online) Temperature dependence of magnetic susceptibility.

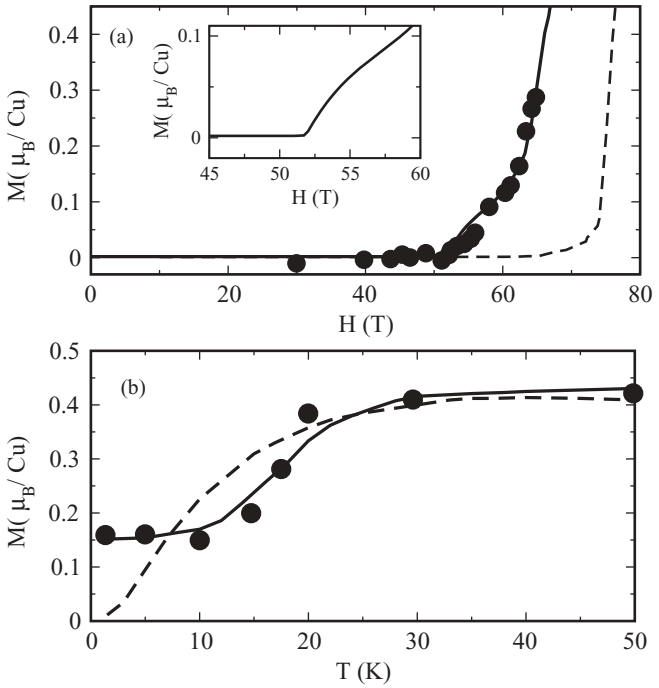

FIG. 10. Magnetization plotted (a) as a function of applied magnetic field at temperature $T = 1.5$ K and (b) as a function of temperature in an applied magnetic field strength $H = 60$ T for dimer model (dotted line) and coupled dimer model (solid line) of $Sr_2Cu(BO_3)_2$. The symbols indicate the experimental data.

where N is the Avogadro number. The QMC simulation of the spin Hamiltonian was carried out by considering a finite lattice of 96×2 sites with periodic boundary conditions, using the stochastic series expansion algorithm.[13–16] We have used 50 000 steps for thermalization and 500 000 steps after thermalization to ensure low statistical errors. To simulate the low-temperature region of the susceptibility data, we have also included the Curie contribution from impurities as $\chi^{CW} = C_{imp}/T$, where $C_{imp} = 0.000\,93$ emu K/mol Oe. The best fit susceptibility for the dimer model ($J_2 = 106.66$ K and $g = 2.13$) and the coupled dimer model ($J_2 = 106.66$ K, $\alpha = 0.125$, and $g = 2.146$) and a comparison with experimental susceptibility is shown in Fig. 9. While the overall agreement of the dimer model as well as the coupled dimer model with the experimental data is good, at the low temperature region (see inset of Fig. 9) the calculated susceptibility with the coupled dimer model has a better agreement with the experimental data. Also the $g = 2.146$ value for the coupled dimer model is in agreement with the average g value obtained from the ESR experiment.[7]

The stochastic series expansion implementation of the quantum Monte Carlo method also allows one to simulate quantum spin models in an external magnetic field. The importance of interdimer coupling is particularly visible in the magnetization versus field and magnetization versus temperature, shown in Figs. 10(a) and 10(b), respectively. Figure 10(a) displays magnetization as a function of field at a very low temperature of 1.5 K. We find that our simulation with the coupled dimer model where $J_2 = 106.66$ K, $\alpha = 0.125$, and $g = 2.146$ is in excellent agreement with the experimental results. We clearly see the upturn in the magnetization occurs at a lower magnetic field than that predicted for a dimer model ($H_c = J_2/g\mu_B = 74.6$ T for $J_2 = 106.66$ K and $g = 2.13$). The characteristic cusplike singularity expected for 1D systems and spin ladders[30,31] is clearly seen in our simulation [see inset of Fig. 10(a)]. This feature is however absent in the experimental data possibly due to anisotropies. The simulation using the isolated dimer model $J_2 = 106.66$ and $g = 2.13$ hardly agrees with the experimental data except for the low field region. Figure 10(b) displays the magnetization as a function of temperature for $H = 60$ T $< J_2/g\mu_B$ (74.6 T). In the same figure we have shown the results obtained from the isolated dimer model and the experimental data. We again find excellent agreement of the result obtained from the coupled dimer model with the experiment. The figure reveals that the magnetization does not fall to zero at low temperature. At higher temperature the $M(T)$ curve rises sharply and coincides with the isolated dimer model. These calculations indicate the reliability of our spin Hamiltonian derived from first-principles electronic structure calculation.

IV. CONCLUSIONS

We have employed *ab initio* density functional calculation using the TB-LMTO and NMTO downfolding method to study the electronic structure of $Sr_2Cu(BO_3)_2$. Calculating various effective hopping integrals we find that the intradimer exchange interaction is dominant and is responsible for the spin gap seen in the system. In contrast to the structural considerations, our *ab initio* calculations reveal that the interdimer interaction is along the crystallographic b direction and is mediated by super-super exchange due to short O-O distances in the exchange pathway. We have derived the relevant spin model for $Sr_2Cu(BO_3)_2$ and the spin model is a system of decoupled spin ladders running along the crystallographic b direction. This spin model was employed to compute magnetic susceptibility as a function of temperature and magnetization as a function of temperature as well as field. At low temperature and high magnetic field our simulations with the coupled dimer model show excellent agreement with the experimental data. Our calculations support that the coupled dimer model is the appropriate model to describe the physics of $Sr_2Cu(BO_3)_2$.

ACKNOWLEDGMENTS

J.C. thanks CSIR, India (Grant No. 09/080(0615)/2008-EMR -1) for research fellowship. I.D. thanks Department of Science and Technology, Govt. of India for financial support.

*sspid@iacs.res.in

[1] P. Lemmens, G. Gntherodt, and C. Gros, Phys. Rep. **375**, 1 (2003).
[2] I. Bose, Curr. Sci. **88**, 62 (2005).
[3] H. Kageyama, K. Yoshimura, R. Stern, N. V. Mushnikov, K. Onizuka, M. Kato, K. Kosuge, C. P. Slichter, T. Goto, and Y. Ueda, Phys. Rev. Lett. **82**, 3168 (1999).

[4]B. S. Shastry and B. Sutherland, Physica B + C **108**, 1069 (1981).
[5]M. Hase, A. Dönni, V. Y. Pomjakushin, L. Keller, F. Gozzo, A. Cervellino, and M. Kohno, Phys. Rev. B **80**, 104405 (2009).
[6]O. Janson, I. Rousochatzakis, A. A. Tsirlin, J. Richter, Y. Skourski, and H. Rosner, Phys. Rev. B **85**, 064404 (2012).
[7]S. E. Sebastian, D. Yin, P. Tanedo, G. A. Jorge, N. Harrison, M. Jaime, Y. Mozharivskyj, G. Miller, J. Krzystek, S. A. Zvyagin *et al.*, Phys. Rev. B **71**, 212405 (2005).
[8]T. Momoi and K. Totsuka, Phys. Rev. B **62**, 15067 (2000).
[9]S. S. Salunke, A. V. Mahajan, and I. Dasgupta, Phys. Rev. B **77**, 012410 (2008).
[10]H. Das, T. Saha-Dasgupta, C. Gros, and R. Valentí, Phys. Rev. B **77**, 224437 (2008).
[11]Y. C. Arango, E. Vavilova, M. Abdel-Hafiez, O. Janson, A. A. Tsirlin, H. Rosner, S.-L. Drechsler, M. Weil, G. Nénert, R. Klingeler *et al.*, Phys. Rev. B **84**, 134430 (2011).
[12]H. J. Koo, D. Dai, and M. H. Whangbo, Inorg. Chem. **44**, 4359 (2005).
[13]A. W. Sandvik, Phys. Rev. B **59**, R14157 (1999).
[14]A. W. Sandvik, AIP Conf. Proc. **1297**, 135 (2010).
[15]O. F. Syljuåsen and A. W. Sandvik, Phys. Rev. E **66**, 046701 (2002).
[16]URL http://physics.bu.edu/∼sandvik/programs/ssebasic/ssebasic.html.
[17]R. Smith and D. A. Keszler, J. Solid State Chem. **81**, 305 (1989).
[18]O. K. Andersen and O. Jepsen, Phys. Rev. Lett. **53**, 2571 (1984).
[19]P. E. Blochl, Phys. Rev. B **50**, 17953 (1994).
[20]G. Kresse and J. Furthmuller, Phys. Rev. B **54**, 11169 (1996).
[21]J. P. Perdew, K. Burke, and M. Ernzerhof, Phys. Rev. Lett. **77**, 3865 (1996).
[22]O. K. Andersen and T. Saha-Dasgupta, Phys. Rev. B **62**, R16219 (2000).
[23]O. K. Andersen, T. Saha-Dasgupta, R. W. Tank, C. Arcangeli, O. Jepsen, and G. Krier, in *Electronic Structure and Physical Properties of Solids. The Uses of the LMTO Method*, edited by H. Dreysse, Springer Lecture Notes in Physics, Vol. 535 (Springer, Berlin, 2000), pp. 3–84.
[24]O. K. Andersen, T. Saha-Dasgupta, and S. Ezhov, Bull. Mater. Sci. **26**, 19 (2003).
[25]E. Zurek, O. Jepsen, and O. K. Andersen, Chem. Phys. Chem. **6**, 1934 (2005).
[26]O. Janson, R. O. Kuzian, S.-L. Drechsler, and H. Rosner, Phys. Rev. B **76**, 115119 (2007).
[27]S. L. Dudarev, G. A. Botton, S. Y. Savrasov, C. J. Humphreys, and A. P. Sutton, Phys. Rev. B **57**, 1505 (1998).
[28]O. Mentré, E. Janod, P. Rabu, M. Hennion, F. Leclercq-Hugeux, J. Kang, C. Lee, M.-H. Whangbo, and S. Petit, Phys. Rev. B **80**, 180413 (2009).
[29]J. Kang, C. Lee, R. K. Kremer, and M.-H. Whangbo, J. Phys.: Condens. Matter **21**, 392201 (2009).
[30]F. Michaud, T. Coletta, S. R. Manmana, J.-D. Picon, and F. Mila, Phys. Rev. B **81**, 014407 (2010).
[31]P. Bouillot, C. Kollath, A. M. Läuchli, M. Zvonarev, B. Thielemann, C. Rüegg, E. Orignac, R. Citro, M. Klanjšek, C. Berthier *et al.*, Phys. Rev. B **83**, 054407 (2011).